25th International Congress on Modelling and Simulation, Darwin, NT, Australia, 9 to 14 July 2023
mssanz.org.au/modsim2023

Statistical analysis of Continuous Haines Index and Fuel Moisture Index for pyrocumulonimbus and non-pyrocumulonimbus wildfires in southeast Australia

C.S. Wilson [a], **W. Ma** [a], **J.J. Sharples** [a,b,c] and **J.P. Evans** [d,e]

[a] *School of Science, University of New South Wales, Canberra*
[b] *NSW Bushfire and Natural Hazards Research Centre*
[c] *ARC Centre of Excellence for Climate Extremes, UNSW Canberra*
[d] *Climate Change Research Centre, University of New South Wales, Sydney*
[e] *ARC Centre of Excellence for Climate Extremes, UNSW Sydney*
Email: caleb.wilson@adfa.edu.au

Abstract: Pyrocumulonimbus (pyroCb) are associated with some of the most extreme wildfire behaviours and some of Australia's most notorious wildfire-related catastrophes. However, while an ever-increasing number of studies continue to shed more light on them, our overall understanding of pyroCb remains relatively limited. As pyroCb have become an increasingly common occurrence in Australia, with over one hundred events observed since 2003, understanding the environments in which they form is a high priority.

In this study, we examined two fire indices in relation to the occurrence of pyroCb: the Continuous Haines Index (C-Haines), consisting of lower-tropospheric stability and dryness components, and the Fuel Moisture Index (FMI), a surface-based index originally developed as a simple alternative for representing fuel moisture content of fine dead fuels. ERA5 reanalysis data (Hersbach et al., 2020) was used to calculate values of C-Haines, its stability and dryness components, and FMI for both large standard (non-pyroCb-producing) wildfires and pyroCb event dates and locations across the southeast Australian mainland at 0200, 0400, and 0600 UTC (12:00, 14:00, and 16:00 AEST). We then explored the distributions of values of C-Haines, its components, and FMI, based on event type (standard wildfire versus pyroCb) and ran statistical tests to see if the two indices possess skill in differentiating pyroCb and standard wildfire environments. Relationships between C-Haines, its components, and FMI were also explored.

We found values of C-Haines, its components, and FMI were all at least slightly skewed, with values tending to be at the more significant end (higher values of C-Haines and its components, lower values of FMI), regardless of event type and time. However, values were significantly more skewed at all three times for pyroCb events. Results of two-sample Kolmogorov-Smirnov tests showed that these differences in distribution were statistically significant at the 99% level.

One concern surrounding the use of C-Haines in Australia is the possibility of the 850-700 hPa layer (used to calculate its stability component) becoming partially or fully engulfed in the planetary boundary layer on very hot, dry days. We therefore investigated pyroCb event dates/locations where the stability component of C-Haines indicated a near-to-super-adiabatic environmental lapse rate. We found a wide variety of surface conditions are associated with these cases, and that this warrants further, more detailed investigation.

Pearson's correlation coefficients were also calculated to explore the relationships between the values of the indices—focusing especially on relationships involving FMI, as C-Haines and FMI are calculated over different levels of the lower troposphere. We found values of C-Haines and its components to be moderately correlated with values of FMI at 0200, 0400, and 0600 UTC. However, when only pyroCb events were considered, these correlations were much stronger.

Results indicate that when a large number of both large standard wildfires and pyroCb events are considered, both C-Haines and FMI show skill in differentiating general pyroCb environments from standard wildfire environments in the southeast Australian mainland. However, further study is needed to explore the relationships between FMI values and values of C-Haines and its stability and dryness components, as well as to explore cases more deeply where the 850-700 hPa temperature difference indicates a near-to-super-adiabatic environmental lapse rate. While this study provides useful information on how general environments differ between standard wildfire and pyroCb events, further study is needed to better-understand meteorological triggers of pyroCb development (fronts, troughs, etc.) and how they relate to the general environments explored here.

Keywords: *Pyrocumulonimbus, wildfire, ERA5 reanalysis, fuel moisture content*

1. INTRODUCTION

Pyrocumulonimbus (pyroCb) are associated with some of the most extreme wildfire behaviours and the most destructive wildfire-related disasters in Australia's long history of catastrophic wildfires (referred to colloquially as bushfires). Notable examples of pyroCb include the firestorms near Lorne, Victoria, and in the Adelaide Hills, South Australia, on Ash Wednesday 1983, the devastating Marysville and Kinglake area firestorms in Victoria on Black Saturday 2009, and the Australian New Year Super Outbreak of pyroCb in Victoria and New South Wales in December and January of 2019-2020 (McRae, 2022; Peterson et al., 2021). However, while each new study about pyroCb provides new insight, our overall understanding of them is still somewhat limited, especially compared to other convective thunderstorm events.

PyroCb have become an increasingly common occurrence in Australia. As of 01 January 2023, 126 pyroCb events have been recorded in the Australian PyroCb Register (McRae, 2022), which dates back to the aforementioned Ash Wednesday fires of 1983. Notably, 120 of those pyroCb events have occurred since the 2002-2003 bushfire season, while 43 occurred in the 2019-2020 fire season alone. As more pyroCb events are studied, researchers are gaining a better idea of the environments in which they form. However, in a nation which regularly experiences high-end fire weather, it can be difficult to differentiate between conditions that encourage fast, linear fire spread from those conducive to convective plume-dominated behaviour.

Here, we have focused on the southeastern Australian states/territories of Victoria, New South Wales (NSW), and the Australian Capital Territory (ACT), as the vast majority of pyroCb events within Australia have been observed there, and as historic wildfires have been relatively well-documented there. We first constructed a dataset of non-pyroCb-producing wildfire events (referred to hereafter as standard wildfires, following the terminology of Di Virgilio et al. (2019)) and pyroCb events for the southeast mainland of Australia. We then used ERA5 reanalysis data (Hersbach et al., 2020) from the European Centre for Medium-Range Weather Forecasts (ECMWF) to calculate values of the Continuous Haines Index (C-Haines), its stability and dryness components, and the Fuel Moisture Index (FMI) for standard wildfire and pyroCb events. We also explored the relationships between each of them.

2. BACKGROUND

Many fire weather indices have been used in Australia to assess the risk of dangerous fire weather conditions. The most well-known is the McArthur Forest Fire Danger Index (FFDI) (McArthur, 1967). FFDI is a surface-based index and although it has been useful in highlighting dangerous surface fire weather conditions, it has been shown to be a poor indicator of pyroCb occurrence, with pyroCb occurrences shown to be spread across a very large range of FFDI values by Di Virgilio et al. (2019). Therefore, FFDI is ignored here in favour of another commonly-used fire weather index in Australia: the Continuous Haines Index (C-Haines, Mills and McCaw, 2010).

C-Haines was developed as a replacement for the original mid-level version of the Haines Index, which was shown to saturate so often across certain parts of Australia, that it is ineffective (Mills and McCaw, 2010). C-Haines allows a larger range of values than the original Haines Index, while still being relatively easy to calculate. C-Haines is made up of two components: a stability component based on the 850-700 hPa temperature difference (CA) and a dryness component based on the 850 hPa dew point depression (CB). C-Haines assumes that greater 850-700 hPa lapse rates and drier conditions at 850 hPa increase the likelihood of "plume-dominated" fire behaviour. The formula for calculating C-Haines and its components is given by (1), (2), and (3).

$$CA = 0.5(T_{850} - T_{700}) - 2; \quad (1)$$

$$CB = 0.3333(T_{850} - Td_{850}) - 1; \quad (2)$$

$$\text{If } T_{850} - Td_{850} > 30\ °\text{C}, \text{then } T_{850} - Td_{850} = 30\ °\text{C};$$

$$\text{If } CB > 5, \text{then CB} = 5 + \frac{(CB-5)}{2};$$

$$C\text{-}Haines = CA + CB. \quad (3)$$

T_{850} is the 850-hPa temperature (°C), T_{700} is the 700-hPa temperature (°C), and Td_{850} is the 850-hPa dew point temperature (°C). The calculation for the CB term also includes two conditional statements in order to prevent the term from growing so large that it dominates the index (Mills and McCaw, 2010). CA is largely bound by the dry adiabatic lapse rate (9.8°C/km), as it is rare for the environmental lapse rate to significantly exceed the dry adiabatic rate. A concern about using 850-700 hPa temperature difference for the original Haines Index's stability component is shared by Mills and McCaw (2010) (raised by Potter (2002)). Potter noted that hot, deep boundary layers could expand into—or entirely engulf—the 850-700 hPa layer, thus possibly casting doubt on the effectiveness of C-Haines. This issue was largely disregarded by Mills and McCaw (2010), as

most of Australia is at lower elevations. However, it should be noted that locations in Southeast Australia with elevations near or exceeding 1500 m are often either very near the 850-700 hPa layer—or within it. For this study, none of the event dates/locations had an analyzed surface pressure below 850 hPa, but several came very close (minimum = 865 hPa).

As hot, dry boundary layers often have near dry adiabatic lapse rates, it is worth noting when CA values become representative of a dry adiabatic lapse rate between 850 and 700 hPa. Mills and McCaw (2010) note that 850-700 hPa lapse values of 15°C to 17°C are representative of a layer that is approximately dry adiabatic. If a 16°C lapse value in (1) is considered, it yields a CA value of 6. This value can be used to identify events where the lapse rate may have been very near-to-super-adiabatic. It is of course important to keep in mind that nearly dry adiabatic lapse rates within the 850-700 hPa layer can occur in other ways as well—such as when relatively cool air is present at the 700 hPa level.

Mills and McCaw (2010) performed extensive analysis of C-Haines for both standard wildfires and pyroCb events through the use of case studies. They showed that C-Haines provides significant insight into plum-dominated fire behaviour that cannot be inferred from surface indices, such as FFDI, alone. Dowdy and Pepler ((2018), Dowdy et al. (2019) and Di Virgilio et al. (2019) all used ERA-Interim reanalysis data to calculate values for C-Haines, dating back to 1979 (the earliest extent of ERA-Interim data). In the latter two studies, values were used to estimate future values of C-Haines across Australia as the climate continues to warm. Additionally, Di Virgilio et al. (2019) also calculated C-Haines and FFDI values for pyroCb events and for a small subset of non-pyroCb "standard" wildfire events in Victoria that burnt greater than 10 ha. Since those studies were published, several factors have changed. Notably, there have been a substantial number of pyroCb and large wildfire events up to, and including, the 2019-2020 fire season. Also, ERA5 reanalysis data is now available at a higher spatiotemporal resolution than its predecessor, presumably allowing for more accurate index calculations.

The FMI (Sharples et al., 2009) was developed as a simpler way to represent the fuel moisture content of fine dead fuels and has the advantage that it is very easy to calculate. Like FFDI, FMI is a surface-based index. However, unlike many other surface-based fire indices, FMI has no wind component. The formula for FMI is shown in (4).

$$FMI = 10 - 0.25(T_{sfc} - RH_{sfc}). \quad (4)$$

T_{sfc} is the surface temperature, while RH_{sfc} is the surface relative humidity. It is important to note that lower values of FMI generally correspond to lower fuel moisture content, and so are meant to indicate conditions more favourable for extreme fire behaviour. It is also important to note that FMI does not relate to soil moisture or drought conditions, and therefore, fuel availability may not be well-captured by its use.

3. DATA AND METHODS

3.1. A standard wildfire and pyroCb event dataset for southeast Australia

To make comparisons between standard wildfire and pyroCb event environments, a single, consistent wildfire dataset for southeast mainland Australia (NSW, ACT, and Victoria) needed to be developed. Victoria (Victoria Department of Environment, Land, Water & Planning 2022) and NSW (including the ACT) (New South Wales Department of Planning and Environment 2022) each have publicly available wildland fire history databases. However, the methods for recording fires and their attributes are inconsistent between the two states. Most of these inconsistencies were relatively easy to rectify, but there were still several challenging issues to work around.

First, many fires, especially those in Victoria, exist as either multi-part (multi-polygon) features or are considered entirely separate records, despite sharing the same attributes (i.e., fire name, number, start date, etc.). Therefore, using GIS software, all multi-part features were first separated, before features were merged based on their common attributes. All events that burnt fewer than 10 ha were then eliminated, as Di Virgilio et al. (2019) had done when similarity looking at Victorian wildfire events.

A second major challenge was that fire start and end dates historically have been inconsistently recorded in NSW/ACT, while only fire start dates are recorded in Victoria. There are also several fires in Victoria and NSW/ACT with no starting dates, while others in Victoria had questionable dates (e.g., large number with 01 January start date). This is problematic since 01 January falls amid the southeast Australian wildfire season. As most of these problematic fires were from many years ago or were very small, simply considering relatively recent fires (e.g., since 1980) and eliminating fires burning fewer than 10 ha, eliminated most fires with 01

January starting dates, while the few that remained could be checked manually. For consistency, fires with no starting date listed were not considered for this dataset.

Using GIS software, the latitude and longitude of the centroid of each fire polygon was determined. Next, pyroCb events from the Australian PyroCb Register were integrated into the combined NSW/ACT/Victoria fire dataset. To avoid double-counting events, standard fires which shared a date with and occurred within the same 0.25° × 0.25° grid cell as a pyroCb event or in an adjacent grid cell., were eliminated from the dataset. Eight wildfires from the standard wildfire dataset met these criteria and were thus classified as pyroCb events and removed from the standard wildfire dataset. Otherwise—to maintain consistency across the dataset—regardless of whether a wildfire ultimately produced a pyroCb in subsequent days, it was counted as a standard wildfire data point, as it did not produce a pyroCb on the day for which C-Haines and FMI were calculated.

The resulting dataset contains the vast majority of recorded fire events in Victoria, NSW, and the ACT since 1980 that burnt at least 10 ha. Although it has its limitations, the resulting southeast Australian standard wildfire and pyroCb event dataset has given us the ability to perform more robust analyses to better-understand both standard wildfire and pyroCb event environments.

To prevent the analysis performed here from being polluted by noisy data from very minor standard wildfire events, a much narrower subset of the southeast Australian standard wildfire and pyroCb event dataset is used. Here, we focus on large standard wildfires that burnt over 1000 ha from 1991 to 2020 (Table 1), as they are more likely to have occurred in conditions that made them difficult enough to initially suppress (e.g., favourable weather conditions and/or terrain). that they were ultimately able to burn more than 1000 ha.

Table 1. Standard wildfire (≥ 1000 ha) and pyroCb events in southeast Australia, 1991-2020.

	State/Territory		
Event Type	NSW/ACT	Victoria	**Total**
Standard	816	170	**986**
PyroCb	40	52	**92**
Total	**856**	**222**	**1078**

3.2. ERA5 reanalysis, calculation of fire weather indices, and statistical tests

ERA5 global reanalysis data from the ECMWF combines observed and modelled data to provide hourly estimates of many meteorological and climatological variables (Hersbach et al., 2020). Among several advantages of ERA5 reanalysis is that it is constrained by large amounts of observed data, and its gridded output is available at a relatively high resolution (0.25° latitude × 0.25° longitude, ~28 km × 28 km). Although not without at least some error, the use of ERA5 reanalysis data has several advantages over relying on observed station and radiosonde data, which in Australia is often taken tens of kilometres (or farther) from fire locations and—in the case of radiosonde data—collected only one to two times daily.

Daily values of C-Haines and FMI were calculated for the locations/dates of standard wildfires and pyroCb-producing fires. For consistency, 0400 UTC (14:00 Australian Eastern Standard time (AEST)) was initially chosen as the time for the daily calculations, as it typically represents a relative peak in fire weather conditions and is consistent with previous studies of Australian fire weather conditions, such as that performed by Di Virgilio et al. (2019).

For FMI calculations (4), 2-m temperature and dewpoint values for each fire date/location were gathered from the ERA5 single level dataset. From these values, relative humidity was calculated, thus allowing FMI values to be calculated. For C-Haines calculations (3), 850 hPa and 700 hPa temperatures and 850hPa relative humidity were obtained from the pressure levels dataset. From these values, 850hPa dewpoint could be calculated, thus allowing for the components of C-Haines and C-Haines itself to be calculated for all fire dates/locations.

We ran a series of two-sample Kolmogorov-Smirnov (K-S) tests to see whether distributions of values of C-Haines, its two components, and FMI differ significantly when considering the type of event (pyroCb versus standard wildfire), as two-sample K-S tests are very useful when dealing with data with skewed distributions. Significant differences in distributions would indicate that C-Haines and FMI possess skill in differentiating the general environments of pyroCb and standard wildfire events. As we were also interested in the relationships between C-Haines, its components, and FMI, we calculated Pearson correlation values for each of those relationships. After reviewing results from 0400 UTC, the process was repeated for 0200 UTC (12:00 AEST) and 0600 UTC (16:00 AEST) to see whether trends we observed at 0400 UTC could be seen at other times as well.

4. RESULTS

4.1. Descriptive statistics and two-sample K-S test results

When plotting C-Haines and its components against each other and against FMI, a few trends are immediately noticeable (Fig. 1). First, value distributions across most variables appear to be at least somewhat skewed, regardless of event type, with the distribution of the CA component (850-700 hPa lapse rate) values appearing to be particularly highly skewed. Second, although distributions are skewed across most variables, the degree to which they are skewed appears to vary based on event type across most, if not all variables. Table 2 shows skewness values—along with other descriptive statistics—for the distributions of values across each variable, based on fire type. For standard wildfires, CB and C-Haines distributions are consistently normal-to-slightly skewed across all times, while FMI and CA are more skewed. However, for pyroCb events, skewness is much greater for all variable value distributions, with most distributions having a skewness greater than +/- 1 across all three times. The skewness of the distribution of CA values for pyroCb events is especially notable, as it increases markedly from -1.35 at 0200 UTC to -2.02 at 0400 UTC. Interestingly, at 0400 UTC, the maximum CA value for pyroCb events is 6.4, yet for 51 of the 92 event dates/locations (55.4%), the value of the CA exceeds the value 6.0 (representative of a near-to-super-adiabatic environmental lapse rate). By comparison, just 13.6% of CA values for large standard wildfire dates/locations exceed 6.0. Table 2 also shows the results of the two-sample K-S tests, which show that based on fire type, differences in the distributions of values of C-Haines, its components, and FMI, are statistically highly significant across all three times.

As mentioned earlier, a concern raised by Mills and McCaw (2010) for the original mid-level Haines Index, as well as for C-Haines, was that the 850-700 hPa layer could be entirely engulfed by the boundary layer on very hot and dry days. Therefore, we looked more closely at surface conditions for the 51 pyroCb event dates/locations with a nearly dry-adiabatic 850-700 hPa temperature lapse at 0400 UTC. We found a wide range of surface temperatures (ranging from 25 °C to 44 °C, mean = 35.5 °C), dew points (ranging from to -3°C to 14°C, mean = 6.9°C), and FMI values (ranging from 1.3 to 11.4, mean = 5.4) for these event dates/locations.

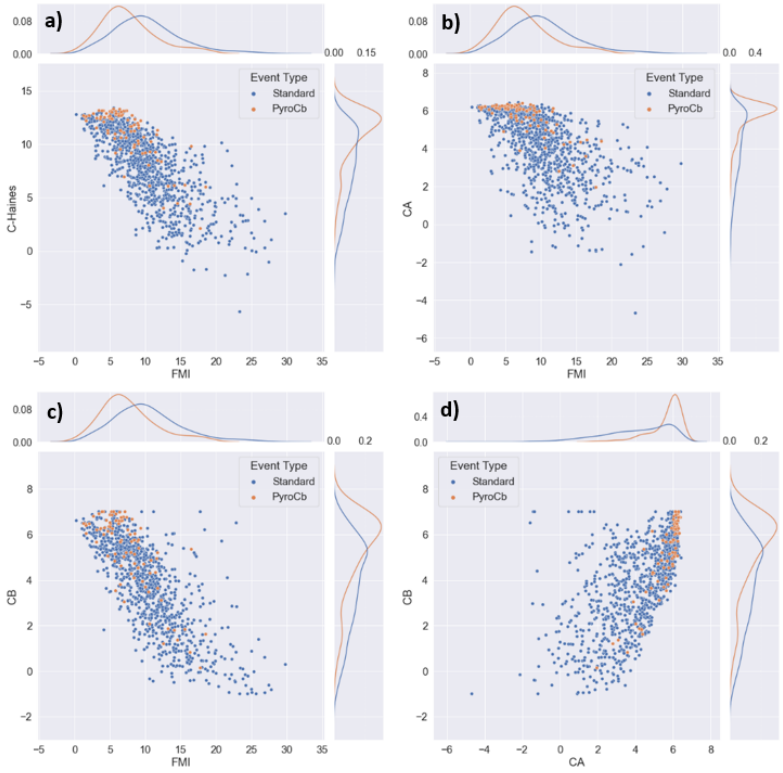

Figure 1. Scatterplots and probability distributions of (a) C-Haines over FMI, (b) CA over FMI, (c) CB over FMI, and (d) CB over CA for large standard wildfire and pyroCb event dates/locations at 0400 UTC (14:00 AEST)

4.2. Pearson correlations of relationships between C-Haines, its components, and FMI

From Figure 1, it is also apparent that values of C-Haines and its components are all at least relatively well-correlated with FMI values. To check the extent of these correlations, Pearson's correlation coefficients for the relationships between each variable (grouped by fire type) were calculated at all three times (Table 3, 0200 and 0600 UTC results are not shown as they are very similar to results from 0400 UTC). Of particular interest are the correlations involving FMI, as it is a surface-based index, while C-Haines and its components are derived from the lower troposphere. All three relationships involving FMI show at least moderate levels of correlation, regardless of event type. Even the relationships between FMI and CA (the stability component), which has no moisture component, are moderately linearly correlated. Interestingly, the correlations involving FMI are even stronger when only pyroCb events are considered.

Table 2. Descriptive statistics and two-sample K-S test results for standard wildfire (≥ 1000 ha) and pyroCb events in southeast Australia, 1991–2020

	Standard (n = 986)					PyroCb (n = 92)					
0200 UTC	M	Md	SD	Skew	Kurt	M	Md	SD	Skew	Kurt	K-S D
C-Haines	7.09	7.42	3.25	-0.46	-0.33	10.30	11.16	2.38	-1.22	0.85	4.168**
CA	3.60	3.92	1.77	-0.78	0.50	5.34	5.58	0.89	-1.35	1.75	4.538**
CB	3.49	3.70	1.91	-0.29	-0.85	4.96	5.57	1.56	-1.12	0.48	3.508**
FMI	10.85	10.35	4.57	0.71	0.89	7.85	7.03	3.61	0.88	0.49	3.331**
0400 UTC	M	Md	SD	Skew	Kurt	M	Md	SD	Skew	Kurt	K-S D
C-Haines	7.87	8.36	3.38	-0.56	-0.36	10.92	11.80	2.49	-1.52	1.79	3.988**
CA	4.09	4.47	1.80	-0.90	0.48	5.65	6.07	0.87	-2.02	4.26	4.227**
CB	3.78	4.05	1.93	-0.44	-0.70	5.26	5.88	1.69	-1.25	0.77	3.712**
FMI	10.32	9.67	4.80	0.81	1.00	7.62	6.70	3.85	0.96	0.82	2.976**
0600 UTC	M	Md	SD	Skew	Kurt	M	Md	SD	Skew	Kurt	K-S D
C-Haines	7.85	8.27	3.45	-0.51	-0.45	10.64	11.88	2.83	-1.28	1.12	3.602**
CA	4.08	4.46	1.82	-0.89	0.43	5.49	5.98	1.03	-1.97	4.47	4.032**
CB	3.77	4.03	1.99	-0.43	-0.77	5.15	5.95	1.88	-1.01	0.14	3.402**
FMI	11.27	10.54	5.37	0.71	0.34	9.49	7.59	5.47	1.15	0.71	2.545**

M = Mean; Md = Median; SD = Standard deviation; Skew = Skewness; Kurt = Kurtosis; K-S D = Kolmogorov-Smirnov D-statistic value; CA = stability component; CB = dryness component
***Indicates significance at the 0.01 level (2-tailed)*

Table 3. Pearson correlations for relationships between C-Haines, its components, and FMI for standard wildfire (≥ 1000 ha) and pyroCb events in southeast Australia, 1991–2020

	Standard (n = 986)				PyroCb (n = 92)			
0400 UTC	C-H	CA	CB	FMI	C-H	CA	CB	FMI
C-Haines	—	.894**	.908**	-.748**	—	.950**	.987**	-.798**
CA	.894**	—	.626**	-.584**	.950**	—	.888**	-.743**
CB	.908**	.626**	—	-.759**	.987**	.888**	—	-.795**
FMI	-.748**	-.584**	-.759**	—	-.798**	-.743**	-.795**	—

C-H = C-Haines; CA = stability component; CB = dryness component
***Indicates the relationship is significant at the 0.01 level (2-tailed)*

5. DISCUSSION AND CONCLUSIONS

A standard wildfire and pyroCb event dataset for southeast Australia was created, from which a smaller subset of large standard fires (greater than 1000 ha burnt) was derived. We used this data to calculate values of C-Haines, its components, and FMI for the dates/locations of standard wildfire and pyroCb events.

A relatively simple look into the data revealed several noteworthy findings. First, we have shown that C-Haines values and FMI values significantly differ between pyroCb and large standard wildfire events in Victoria, NSW, and the ACT, with higher values of C-Haines and lower values of FMI tending to occur for pyroCb event dates/locations compared to standard wildfire dates/locations. This shows that C-Haines and FMI possess skill in differentiating general pyroCb environments from those associated with standard wildfires. It also supports the results of studies by Mills and McCaw (2010) and Di Virgilio et al. (2019), which suggested such for C-Haines while using different approaches and sources of input data. The results for FMI are interesting, as it is an entirely surface-based index with just two input variables: surface temperature and relative humidity (meaning surface temperature is actually double-represented in its calculation). Nevertheless, the differences based on fire event type are obvious and significant. It is also worth noting that these observed statistical differences between values of C-Haines, its components, and FMI, based on event type, are present during all three times for which they were measured—0200, 0400, and 0600 UTC (12:00, 14:00, and 16:00 AEST), indicating that these are characteristics that tend to persist throughout much of the afternoon of wildfire event days.

A second finding of interest is the relatively strong correlations of FMI with C-Haines and its components, especially with respect to CA (the stability component), as the two share no common input variables and the measurements are taken from different locations within the troposphere. That CA and FMI are more strongly correlated for pyroCb event dates/locations is also significant and warrants further study. The highly-skewed and very condensed distribution of CA values for pyroCb event dates/locations is also intriguing. A near-to-super-adiabatic value of CA is 6.0, and yet 74% of CA values for pyroCb event dates/locations at 0400 UTC exceeded that value, which was not expected. Furthermore, we found that a nearly dry-adiabatic 850-700 hPa layer is not necessarily indicative of the layer being engulfed by a hot, dry boundary layer, as a closer look at pyroCb event dates/locations where the CA value exceeded 6 revealed a variety of surface conditions—ranging

from extremely hot to relatively cool and from very dry to relatively moist. While we understand that we may have missed the timing of a few of the actual pyroCb events (those occurring outside of the 0200-0600 UTC window), and may have instead sampled a changed lower troposphere, what is more relevant is understanding that CA values (and in turn C-Haines values) can be very high, even when surface fire weather conditions may be less favourable due to diurnal cooling and rising humidity and/or the intrusion of cooler and moister air near the surface from a shallow trough passage.

A limitation of this analysis is the use of start dates of standard wildfire events due to the data consistency issues within the state wildfire databases. There is a possibility that individual wildfires would have experienced more severe fire weather conditions in subsequent days without pyroCb formation. However, without consistently recorded ending dates, this cannot be confirmed. We attempted to alleviate some of this concern through the selection of only relatively large standard wildfires, and we are confident in our findings given the stark difference in distributions of C-Haines and FMI between standard wildfire and pyroCb events. However, further work is needed to continue to develop methods to make effective use of historical wildfire data in Australia, as it is too valuable of a resource not to be utilised.

Further research is also needed to determine if other near-surface and troposphere-based fire weather indices, such as the Hot-Dry-Windy Index (Srock et al., 2018) and Pyrocumulonimbus Firepower Threshold (Tory and Kepert, 2021) possess skill in differentiating pyroCb and standard wildfire environments Finally, while this study provides useful information on how general environments differ between standard wildfire and pyroCb events, further study is needed to better-understand other meteorological factors and triggers associated with pyroCb development (fronts, troughs, etc.) and how they relate to the general environments explored here.

ACKNOWLEDGEMENTS

We would like to acknowledge the contributions of Rick McRae, whose conversations helped shape the direction of this research. Funding for this research has been provided to C.S. Wilson and W. Ma by UNSW international postgraduate research scholarships. This research was undertaken with the assistance of resources and services from the National Computational Infrastructure (NCI), which is supported by the Australian Government.

REFERENCES

Di Virgilio, G., Evans, J.P., Blake, S.A.P., Armstrong, M., Dowdy, A.J., et al., 2019. Climate Change Increases the Potential for Extreme Wildfires. Geophysical Research Letters 46, 8517–8526. https://doi.org/10.1029/2019GL083699

Dowdy, A.J., Pepler, A., 2018. Pyroconvection Risk in Australia: Climatological Changes in Atmospheric Stability and Surface Fire Weather Conditions. Geophysical Research Letters 45, 2005–2013. https://doi.org/10.1002/2017GL076654

Dowdy, A., Ye, H., Pepler, A., Thatcher, M., Osbrough, S., et al., 2019. Future changes in extreme weather and pyroconvection risk factors for Australian wildfires. Scientific Reports 9. https://doi.org/10.1038/s41598-019-46362-x

Hersbach, H., Bell, B., Berrisford, P., Hirahara, S., Horányi, A., et al., 2020. The ERA5 global reanalysis. Quarterly Journal of the Royal Meteorological Society 146, 1999–2049. https://doi.org/10.1002/qj.3803

McArthur, A.G., 1967. Fire behaviour in eucalypt forests. Department of National Development Forestry and Timber Bureau, Canberra.

McRae, R.H.D., 2022. Australian PyroCb Register [WWW Document]. URL https://www.highfirerisk.com.au/pyrocb/register.htm (accessed 8.4.22).

Mills, G.A., McCaw, W.L., 2010. Atmospheric stability environments and fire weather in Australia: extending the Haines index. Centre for Australian Weather and Climate Research, Melbourne.

Peterson, D.A., Fromm, M.D., McRae, R.H.D., Campbell, J.R., Hyer, E.J., et al., 2021. Australia's Black Summer pyrocumulonimbus super outbreak reveals potential for increasingly extreme stratospheric smoke events. npj Clim Atmos Sci 4, 1–16. https://doi.org/10.1038/s41612-021-00192-9

Potter, B.E., 2002. A dynamics based view of atmosphere-fire interactions. International Journal of Wildland Fire 11:247-255 11.

Sharples, J.J., McRae, R.H.D., Weber, R.O., Gill, A.M., 2009. A simple index for assessing fuel moisture content. Environmental Modelling & Software 24, 637–646. https://doi.org/10.1016/j.envsoft.2008.10.012

Srock, A., Charney, J., Potter, B., Goodrick, S., 2018. The hot-dry-windy index: A new fire weather index. Atmosphere 9, 279. https://doi.org/10.3390/atmos9070279

Tory, K.J., Kepert, J.D., 2021. Pyrocumulonimbus Firepower Threshold: Assessing the Atmospheric Potential for pyroCb. Weather and Forecasting 36, 439–456. https://doi.org/10.1175/WAF-D-20-0027.1